Static magnetic order in the triangular lattice of Li_xNiO_2 ($x \leq 1$): Muon-spin spectroscopy measurements

Jun Sugiyama,[1,*] Kazuhiko Mukai,[1] Yutaka Ikedo,[1] Peter L. Russo,[2] Hiroshi Nozaki,[1] Daniel Andreica,[3] Alex Amato,[3] Kingo Ariyoshi,[4] and Tsutomu Ohzuku[4]

[1]*Toyota Central Research and Development Laboratories Inc., Nagakute, Aichi 480-1192, Japan*

[2]*TRIUMF, 4004 Wesbrook Mall, Vancouver, British Columbia, V6T 2A3 Canada*

[3]*Laboratory for Muon Spin Spectroscopy, Paul Scherrer Institut, CH-5232 Villigen PSI, Switzerland*

[4]*Department of Applied Chemistry, Graduate School of Engineering, Osaka City University, Osaka 558-8585, Japan*

(Received 14 July 2008; published 10 October 2008)

In spite of numerous experimental and theoretical reports on $LiNiO_2$, no consistent picture has emerged of the nature of its ground state. We have investigated the Li_xNiO_2 system ($0.1 \leq x \leq 1$) by means of muon-spin spectroscopy and susceptibility to gain further insight from the effects of varying the magnetic ion concentration. Static magnetic order, most likely to be incommensurate to the spatial lattice period, was found for $x \geq 0.6$ at low temperatures (T), while disordered magnetism due to localized Ni moments appears for $x = 1/2-1/4$ and, finally, $Li_{0.1}NiO_2$ exhibits almost fully nonmagnetic behavior down to the lowest T measured. The ground state of $LiNiO_2$ is inferred to be a "static but short-range" A-type antiferromagnetic ordered system, in which the Ni^{3+} moments align ferromagnetically along the c axis in the NiO_2 plane with an incommensurate modulation probably due to canting of the Ni^{3+} moments, but align antiferromagnetically between adjacent NiO_2 planes.

DOI: 10.1103/PhysRevB.78.144412 PACS number(s): 76.75.+i, 75.30.Fv, 75.50.Ee, 75.50.Lk

I. INTRODUCTION

The two-dimensional triangular lattice (2DTL) antiferromagnet at half-filling has been investigated for an extended time both experimentally and theoretically because of the richness of its physics resulting from competition between the antiferromagnetic (AF) interaction and geometrical frustration. In the rhombohedral $LiNiO_2$ lattice with space group $R\bar{3}m$ (see Fig. 1), the NiO_2 planes and Li layers form alternating stacks along the c_H axis in a hexagonal setting. In the NiO_2 planes, Ni ions form a 2DTL by a network of edge-sharing NiO_6 octahedra. Since the 2DTL planes are separated by nonmagnetic Li layers and Ni^{3+} is in the low spin state ($t_{2g}^6 e_g^1$) with $S=1/2$, $LiNiO_2$ is thought to be an ideal material for elucidating frustrated magnetism on a half-filled 2DTL. Despite the half-filled state, $LiNiO_2$ exhibits p-type semiconductivity in the whole temperature (T) range measured between 180 and 970 K.[1,2] In early work, it was proposed that Ni^{3+} spins behave Ising-type with an easy axis along the c_H direction.[3] Thus far, no long-range magnetic order has been detected down to the lowest T investigated,[3–6] although the susceptibility (χ) shows a spin-glass-like (SG-like) anomaly around 10 K.[7] Both heat capacity and NMR measurements, however, suggest a spin-liquid state with short-range ferromagnetic (FM) correlations.[4] Positive muon-spin rotation and relaxation (μ^+SR) experiments have also indicated the absence of static magnetic order down to 2 K as well as showing the existence of fast fluctuating moments.[5] Recent neutron-diffraction (ND) experiments have also raised the possibility of local-orbital ordering of Ni^{3+} into three sublattices.[6]

Past work revealed that the excess Ni is usually present in the Li layer of the $LiNiO_2$ samples[7–9] due to the similarity in ionic radii between Li^+ and Ni^{3+}. The ionic distribution of the Ni-excess $LiNiO_2$ is thus given as $[Li_{1-z}^+ Ni_z^{2+}]_{3b}[Ni_{1-z}^{3+} Ni_z^{2+}]_{3a}[O_2]_{6c}$,[8] where Li ions occupy $3b$, Ni ions $3a$, and O ions $6c$ sites in the regular $LiNiO_2$ lattice. The Ni^{2+} ions at the $3b$ site are known to introduce an additional interplane interaction, which alters the low-T magnetism from the spin-glass-like state below ~10 K ($=T_m$) for $z \sim 0$ to the ferro- or ferrimagnetic state at ~100 K for $z \geq 0.04$.[7,10] In spite of efforts to prepare it, fully stoichiometric $LiNiO_2$ (Refs. 10 and 11) is still unavailable and, as a result, the ground state of $LiNiO_2$ continues to be under discussion.[12]

The other layered nickel dioxides with a 2DTL such as rhombohedral $NaNiO_2$,[13–15] $AgNiO_2$,[16–18] and Ag_2NiO_2 (Refs. 19 and 20) have also been investigated in order to clarify the ground state of the NiO_2 plane. However, it is currently not possible to understand the nature of these compounds as a whole by a common physics framework.[21–25] That is, $NaNiO_2$ exhibits two transitions at $T_{JT} \sim 480$ K and $T_N = 20$ K. The former is a cooperative Jahn-Teller (JT) transition from a high-T rhombohedral phase to a low-T monoclinic phase, while the latter is a transition into an A-type AF phase, since ND and μ^+SR experiments have shown ferromagnetic (FM) order in the NiO_2 plane but AF order between

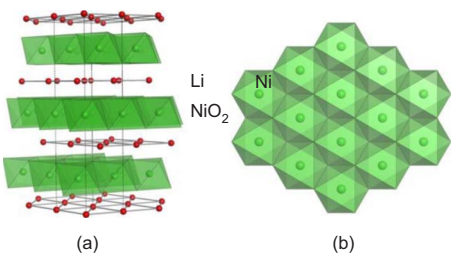

FIG. 1. (Color online) Crystal structure of $LiNiO_2$. (a) Alternating stacks along the c_H axis and (b) triangular lattice in the c_H plane (NiO_2 plane).

adjacent NiO_2 planes.[13–15] In contrast, $AgNiO_2$ lacks a cooperative JT transition but has a long-range commensurate (C) AF ordered state with $T_N=21$ K caused by slight spatial deviation of the O^{2-} ions, as was recently found by ND and μ^+SR measurements.[17,18] For $(Ag_2)^+Ni^{3+}O_2$, which also keeps a rhombohedral symmetry down to 2 K, static AF order, likely the formation of an incommensurate spin-density wave (IC-SDW) structure in the NiO_2 plane, was observed below $T_N=56$ K by a recent μ^+SR experiment.[20]

In order to further elucidate the nature of the NiO_2 plane and resolve the current confusing situation (see the introduction of Ref. 6, for example), we have chosen another approach to this subject, namely, to clarify the change in magnetism associated with changes of the valence of Ni ions, in other words, to know the variation of magnetism with the spin concentration on the 2DTL. For $LiNiO_2$, Li ions are easily deintercalated by electrochemical reaction down to $x\sim 0$ and, in fact, $LiNiO_2$ has been heavily investigated as a next generation cathode material of Li-ion batteries.[26,27] The majority of previous research into Li_xNiO_2 has focused primarily on their structural and electrochemical properties with the aim of understanding their influence on the charge or discharge characteristics of Li-ion batteries. No systematic studies of the magnetic nature of Li_xNiO_2 at low T have been carried out thus far, although ^{7}Li-NMR results in the T range above 263 K have recently become available.[28]

In this paper, we describe our study of the microscopic magnetic nature of Li_xNiO_2 with $x=1$, 3/4, 2/3, 3/5, 1/2, 1/3, 1/4, and 0.1 by means of μ^+SR, which is very sensitive to the local magnetic and structural environments, because the implanted μ^+'s response is dominated by the magnetic field generated by their nearest neighbors. We will discuss the μ^+SR results in conjunction with bulk susceptibility measurements on the same samples. We demonstrate the existence of a variety of phases as a function of x in Li_xNiO_2. In particular, the appearance of static magnetic order, most likely incommensurate (IC) order for Li_xNiO_2 with $x=1$, 3/4, 2/3, and 3/5, suggests the A-type AF ordered state with an IC modulation in the plane for the ground state of the NiO_2 triangular lattice.

II. EXPERIMENTAL

A powder sample of $LiNiO_2$ was prepared at Osaka City University by a solid-state reaction technique using reagent grade $LiOH*H_2O$ and NiO powders as starting materials. A mixture of the two powders was heated at 750 °C for 12 h in an oxygen flow. Powder x-ray diffraction (XRD) analysis showed that the sample was single phase with a rhombohedral system of space group $R\bar{3}m$ ($a_H=0.2875$ and $c_H=1.4191$ nm in a hexagonal setting). In order to estimate the excess Ni in the Li plane, χ was measured below 400 K under a $H\leq 10$ kOe field with a superconducting quantum interference device (SQUID) magnetometer (MPMS, Quantum Design) for two powders (A and B) from another lot. Their Weiss temperature (Θ) and effective magnetic moment (μ_{eff}) were determined from $\chi(T)$ using a Curie-Weiss law in the range between 80 and 400 K to be 39–46 K and 2.04–2.08 μ_B, respectively [see Figs. 2(a) and 2(b)]. In addition, the $\chi(T)$ curve obtained with $H=100$ Oe exhibits a clear cusp at 11 K ($=T_m$), as seen in Fig. 2(c). Since these values are in good agreement with those reported for $[Li_{1-z}Ni_z]NiO_2$ with $z\leq 0.02$,[7,10,29] z for the present samples is estimated as ~ 0.02.

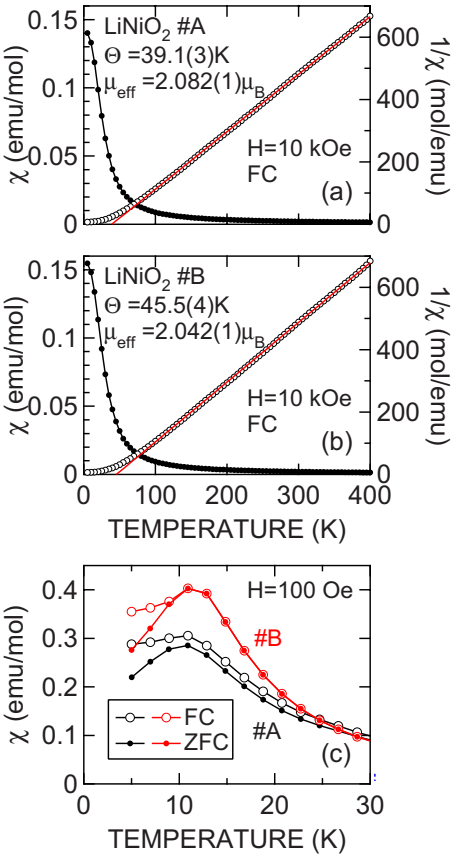

FIG. 2. (Color online) T dependences of the susceptibility (χ) for two $LiNiO_2$ samples (A and B) from another lot. (a) and (b) The $\chi(T)$ and $1/\chi(T)$ curves obtained in FC mode with $H=10$ kOe and (c) the $\chi(T)$ curve obtained in both FC and zero-field cooling (ZFC) mode with $H=100$ Oe. Red lines in (a) and (b) represent a linear fit in the T range between 80 and 400 K using a Curie-Weiss formula $\chi=C/(T-\Theta)$ and $C=(Ng^2\mu_B^2/3k_B)\mu_{\text{eff}}^2$. Here, N is the number density of Ni spins, g is the Landé g factor, μ_B is the Bohr magneton, and k_B is Boltzmann's constant. We assumed $g=2$.

The Li-deficient samples were prepared by an electrochemical reaction using $Li|LiPF_6$-ethylene carbonate-dimethyl carbonate$|LiNiO_2$ cells. The $LiNiO_2$ powder was pressed into a disk with 15 mm diameter and 0.4 mm thickness and the disk was used as a positive electrode. The Li_xNiO_2 disk was removed from the cell in a He-filled glove box just before the μ^+SR measurement and then packed into a sealed powder cell. In order to assess possible changes in the Li-deficient samples during the μ^+SR measurement, each sample was returned to the original cell afterwards to check their voltage (vs Li electrode). No significant change in the voltage, before and after the measurements, was observed. Their structures were subsequently confirmed by powder XRD and, finally, their compositions were checked by an induction-coupled plasma (ICP) analysis. The above procedure is essentially the same as that of our recent μ^+SR work

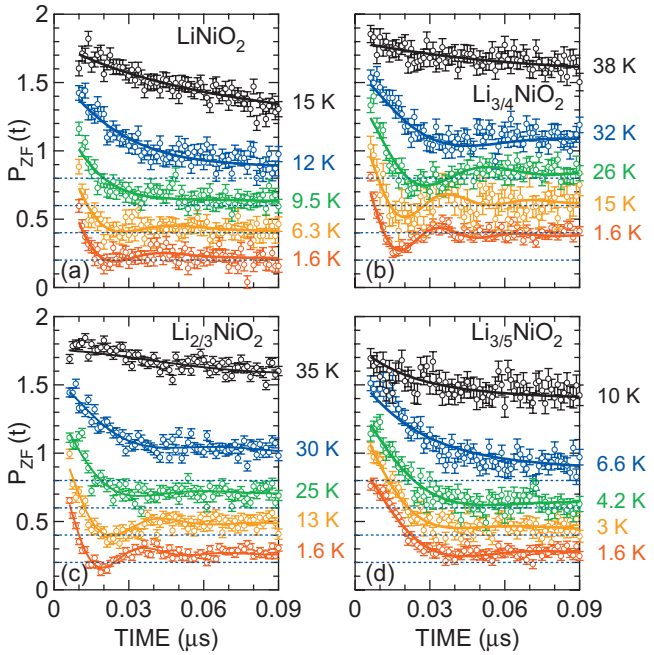

FIG. 3. (Color) Temperature dependence of zero-field μ^+SR spectra for Li_xNiO_2 with $x=1$, 3/4, 2/3, and 3/5 [from (a) to (d)]. Solid lines represent the fit results using Eq. (1). Each spectrum is offset by 0.2 for clarity of display. The composition (Li/Ni ratio) determined by an ICP analysis is [from (a) to (d)] 0.97, 0.75, 0.65, and 0.61, respectively.

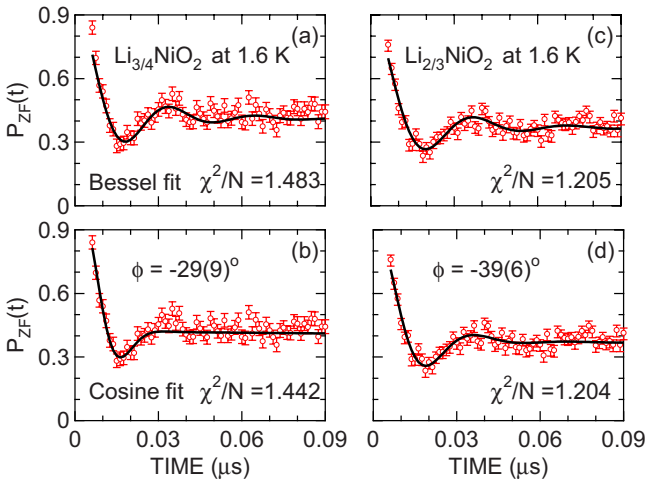

FIG. 4. (Color online) Fit results of the ZF-μ^+SR spectrum for (a) and (b) $Li_{3/4}NiO_2$ and (c) and (d) $Li_{2/3}NiO_2$ at 1.6 K. The fit using a Bessel function (J_0) for an incommensurate order [(a) and (c)] provides a reasonable result, while the fit using a cosine oscillation [(b) and (d)] gives almost the same result as that of the Bessel function, but the obtained delay of the initial phase ($\phi\sim-30°$–$-40°$) is physically meaningless. Since the fit was performed to minimize χ^2, reduced χ^2 ($=\chi^2/N$) is shown for comparison, where N is degree of freedom. There are eight parameters in Eq. (2), whereas seven parameters in Eq. (1). The cosine fit thus yields slightly better reduced χ^2 than the Bessel fit.

on Li_xCoO_2.[30] The μ^+SR experiments were performed on the π-**E1** and π-**M3** surface muon beam lines at PSI using an experimental setup and techniques described elsewhere.[31]

III. RESULTS

A. Li_xNiO_2 with $3/5 \leq x \leq 1$

Figures 3(a)–3(d) show the zero-field (ZF) μ^+SR spectra at several temperatures for the four Li_xNiO_2 samples with $x \geq 3/5$ in the time domain up to 0.1 μs. Although the spectra for $LiNiO_2$ and $Li_{3/5}NiO_2$ exhibit only a first minimum around 0.025 and 0.04 μs, respectively, even at 1.6 K, the spectra for $Li_{3/4}NiO_2$ and $Li_{2/3}NiO_2$ clearly show two minima, unambiguously confirming a damped oscillation. The oscillation signal in a ZF spectrum, even if it is strongly damped, clearly signifies the appearance of static magnetic order in $Li_{3/4}NiO_2$ and $Li_{2/3}NiO_2$. We should note that, as x decreases from 1, the second minimum clearly appears in the ZF spectrum for $x=3/4$ and $x=2/3$ at low T, but it has only the first minimum at $x=3/5$. This clearly demonstrates the effect of a competition between the magnetic interaction and spin concentration on static magnetic order. In other words, the ZF spectra for $LiNiO_2$ and $Li_{3/5}NiO_2$ should be explained by the same physics as those for $Li_{3/4}NiO_2$ and $Li_{2/3}NiO_2$.

Although the oscillating spectra can be fitted by a strongly damped cosine oscillation $[\exp(-\lambda t)\times\cos(\omega_\mu t+\phi)]$ due to static and C-AF order with wide field distribution, it is more reasonable to fit them by a zeroth-order Bessel function of the first kind $[J_0(\omega_\mu t)]$, which accounts for explaining the fast relaxing behavior in the early time domain (before 0.05 μs) and, more importantly, the extra $30°$–$40°$ delay of the initial phase (ϕ) required in the cosine fit for Li_xNiO_2 with $x=3/4$ and 2/3 (see Fig. 4). Here, the ZF spectrum described by J_0 is the well established signature that the μ^+s experience an IC magnetic field in the lattice,[31] though there is a rare exception.[32] More precisely, the ZF-μ^+SR spectra at low T were fitted with a combination of three signals

$$A_0 P_{ZF}(t) = A_{IC} e^{-\lambda_{IC} t} J_0(\omega_{IC} t) + A_{fast} e^{-\lambda_{fast} t} + A_{slow} e^{-\lambda_{slow} t}, \quad (1)$$

where A_0 is the maximum muon decay asymmetry, A_{IC}, A_{fast}, and A_{slow} are the asymmetries of the J_0 signal due to static IC-AF order, a fast exponentially relaxation signal due to fluctuating moments which gives only minor contributions, and a slow exponentially relaxation signal due to the "1/3 tail" caused by the AF component parallel to the initial muon-spin polarization (plus an offset signal from the μ^+'s stopped in the sample cell for Li_xNiO_2 with $x<1$), respectively. λ_{IC}, λ_{fast}, and λ_{slow} are the relaxation rates of the corresponding signals.

While the ZF spectrum for the $x=3/4$ and 2/3 samples exhibits a clear damped oscillation at 1.6 K, the spectrum for the $x=1$ and 3/5 samples is so strongly damped that one can be sure only that the Ni moments freeze in a highly disordered fashion. We thus attempted to fit the ZF spectrum for $LiNiO_2$ using other possible functions, instead of J_0 in Eq. (1), namely, a damped cosine function, as in the case for the $x=3/4$ and 2/3 samples, and a dynamic Gaussian Kubo-Toyabe (KT) function $G^{DGKT}(t,\Delta,\nu)$ for a fluctuating disordered phase

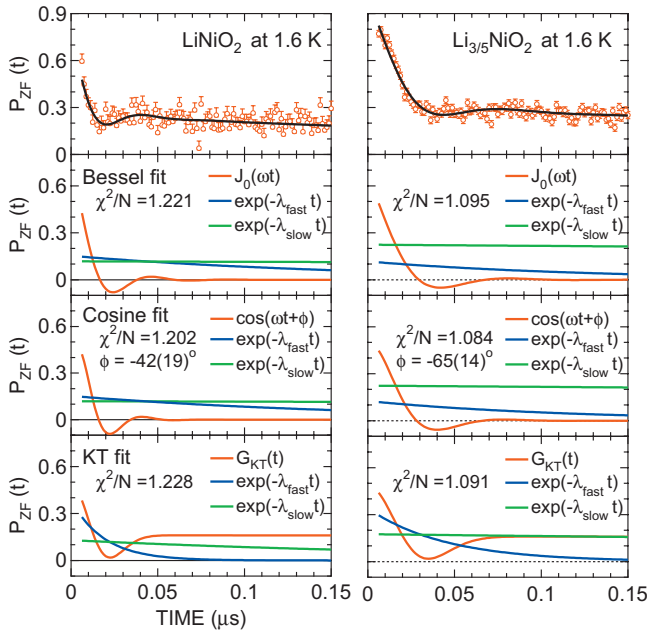

FIG. 5. (Color) Fit results of the ZF-μ^+SR spectrum for (left) $LiNiO_2$ (B) and (right) $Li_{3/5}NiO_2$ at 1.6 K. Note that a Kubo-Toyabe function for a random disordered phase needs an additional fast relaxing component $[\exp(-\lambda_{fast}t)]$ with almost the same amplitude to that of the KT component (see Table I).

$$A_0 P_{ZF}(t) = A_{AF} e^{-\lambda_{AF} t} \cos(\omega_{AF} t + \phi) + A_{fast} e^{-\lambda_{fast} t} + A_{slow} e^{-\lambda_{slow} t}, \tag{2}$$

$$A_0 P_{ZF}(t) = A_{KT} G^{DGKT}(t, \Delta, \nu) + A_{fast} e^{-\lambda_{fast} t} + A_{slow} e^{-\lambda_{slow} t}, \tag{3}$$

where A_{AF} and A_{KT} are the asymmetries of the C-AF and KT signals, λ_{AF} is the relaxation rates, ω_{AF} is the muon Larmor frequency for the C-AF ordered field, ϕ is the initial phase of the precession, Δ is the static width of the local frequencies at the disordered sites, and ν is the field fluctuation rate. When $\nu=0$, $G^{DGKT}(t,\Delta,\nu)$ is a static Gaussian Kubo-Toyabe function $G_{zz}^{KT}(t,\Delta)$ given by

$$G_{zz}^{KT}(t,\Delta) = \frac{1}{3} + \frac{2}{3}(1-\Delta^2 t^2) e^{-\Delta^2 t^2/2}. \tag{4}$$

The fit results using Eqs. (1)–(3) are shown in Fig. 5 and the obtained parameters are listed in Table I. The KT fit yields that $\Delta = 76.88(1) \times 10^6$ s^{-1} and $\nu = 0.18(5) \times 10^6$ s^{-1} for $LiNiO_2$ [$\Delta = 49.7(3) \times 10^6$ s^{-1} and $\nu = 0.17(4) \times 10^6$ s^{-1} for $Li_{3/5}NiO_2$], indicating the static nature of the disordered field because $\Delta \gg \nu$. This is inconsistent with the past high-longitudinal field μ^+SR result.[5] Moreover, the fact that $A_{fast}/A_{KT} \sim 0.8$ for $LiNiO_2$ (~ 0.7 for $Li_{3/5}NiO_2$) in turn provides two possibilities: one is that there are two magnetically inequivalent muon sites in the lattice and the other is coexistence of two different magnetic phases in the sample at low T. If there are two inequivalent muon sites in the $LiNiO_2$ lattice, the magnetic environment responsible for the A_{KT} signal is static, whereas that for the A_{fast} signal is dynamic. Such a situation is very unlikely to be applicable for the $LiNiO_2$ lattice because of the short distance between the two adjacent NiO_2 planes. Furthermore, electrostatic potential calculations suggest that muons locate at the vicinity of O^{2-} ions, as in the case for $LiCoO_2$ (Ref. 30) and $NaNiO_2$.[15] This also excludes the possibility that the two magnetically different muon sites coexist in the $LiNiO_2$ lattice. On the other hand, concerning the possibility of an intrinsic phase separation at low T, there are no evidences in past NMR measurements.[4] In addition, the ratio A_{fast}/A_{KT} for $LiNiO_2$ is comparable to that for $Li_{3/5}NiO_2$, although the ratio would be expected to depend on x, if we assume the reaction $Li_xNiO_2 \rightarrow yLi_{x1}NiO_2 + (1-y)Li_{x2}NiO_2$ ($x1 > x > x2$) for both samples. As a result, the KT fit is most unlikely to explain the magnetic nature of $LiNiO_2$ and $Li_{3/5}NiO_2$. The cosine

TABLE I. Parameters obtained by fit of the ZF-μ^+SR spectrum for $LiNiO_2$ and $Li_{3/5}NiO_2$ at 1.6 K using Eqs. (1)–(3). A_{main} is A_{IC} for Eq. (1), A_{AF} for Eq. (2), and A_{KT} for Eq. (3).

Equation	A_{main}	A_{fast}	λ_{fast} (10^6 s^{-1})	A_{slow}	λ_{slow} (10^6 s^{-1})	χ^2/N
			$LiNiO_2$, A			
(1) J_0	0.1690(8)	0.03480(2)	9.66(11)	0.0362(8)	0.507(2)	266.89/212=1.259
(2) cos	0.166(2)	0.038(2)	11.0(1.3)	0.036(4)	0.52(4)	269.46/211=1.277
(3) G^{DGKT}	0.1018(2)	0.1157(2)	56.0(1.8)	0.0225(4)	4.5(3)	238.95/212=1.127
			$LiNiO_2$, B			
(1) J_0	0.175(4)	0.037(2)	6.1(8)	0.028(6)	0.25(7)	258.88/212=1.221
(2) cos	0.175(4)	0.037(3)	6.0(8)	0.033(3)	0.28(7)	253.70/211=1.202
(3) G^{DGKT}	0.116(2)	0.092(10)	53(4)	0.03(1)	4.1(2)	260.29/212=1.228
			$Li_{3/5}NiO_2$			
(1) J_0	0.158(3)	0.028(4)	7.9(1.4)	0.054(1)	0.34(3)	232.08/212=1.095
(2) cos	0.156(3)	0.030(3)	8.7(1.2)	0.033(3)	0.35(3)	228.62/211=1.084
(3) G^{DGKT}	0.116(5)	0.082(4)	22(2)	0.03(1)	0.71(9)	231.32/212=1.091

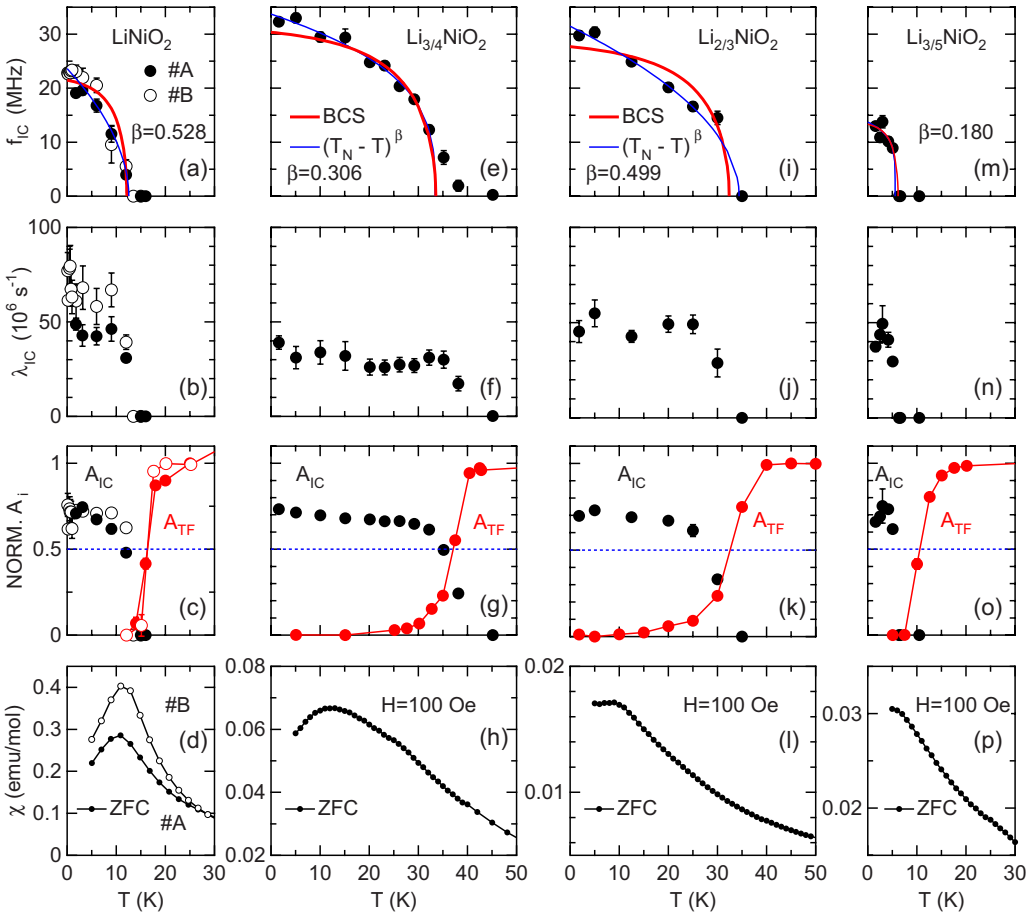

FIG. 6. (Color online) Temperature dependences of (a), (e), (i), and (m) the muon precession frequency ($f_{IC} \equiv \omega_{IC}/2\pi$), (b), (f), (j), and (n) the exponential relaxation rate λ_{IC}, (c), (g), (k), and (o) the normalized A_{IC} and A_{TF}, and (d), (h), (l), and (p) χ for $LiNiO_2$, $Li_{3/4}NiO_2$, $Li_{2/3}NiO_2$, and $Li_{3/5}NiO_2$, respectively. The data were obtained by fitting the ZF spectrum using Eq. (1) and the wTF spectrum using an exponential damped cosine oscillation $A_{TF}\exp(-\lambda_{TF}t)\cos(\omega_{TF}t+\phi)$. The red solid line in (a), (e), (i), and (m) represents the T dependence of the BCS gap energy, as expected for the order parameter of the IC-AF state (Ref. 33). The blue line, on the other hand, represents the fitting result using the equation $f/f_0=[(T_N-T)/T_N]^{\beta}$ for the commensurate ordered phase; since $\beta=0.528$ for $LiNiO_2$, 0.306 for $Li_{3/4}NiO_2$, 0.499 for $Li_{2/3}NiO_2$, and 0.180 for $Li_{3/5}NiO_2$, it is difficult to explain the $f(T)$ curve for the above four samples by a common phenomenology if we assume the C-ordered phase. χ was measured in ZFC mode with $H=100$ Oe. Note that there is no significant change in the μ^+SR parameters for the $x=3/4$ and 2/3 samples at ~ 10 K, at which the $\chi_{ZFC}(T)$ curve exhibits a clear cusp [see (h) and (l)].

oscillation model provides almost the same goodness of fit than the Bessel function, but the obtained delay of the initial phase ($\phi \sim -40 - -60°$) is physically meaningless. This indicates that the cosine fit is unsuitable in this case.

Although it is very hard to infer whether the traces of order reflect IC-, C-AF tendencies, or a Kubo-Toyabe behavior for $LiNiO_2$ based only on the present results, the fits to a critically damped IC-AF give an overall more reasonable explanation for the magnetism of Li_xNiO_2. Unfortunately, μ^+SR provides no information on the correlation length of static magnetic order. However, since both NMR and neutron measurements showed an absence of long-range order for $LiNiO_2$, the static order detected by μ^+SR is likely to be "short-ranged" from the NMR and/or neutron-diffraction viewpoint.

Figure 6 shows the T dependences of the μ^+SR parameters for the two $LiNiO_2$ samples (A and B of Fig. 2) and the Li_xNiO_2 samples with $x=3/4$, 2/3, and 3/5 obtained from the ZF and weak transverse field (wTF) data with wTF=30 Oe. Since the normalized wTF asymmetry ($N_{A_{TF}}$) is roughly proportional to the volume fraction of paramagnetic phases, it is found that the whole sample enters into the magnetic phase below ~ 16 K ($=T_N^{mid}$, at which $N_{A_{TF}}=0.5$) for $LiNiO_2$, ~ 37 K for $Li_{3/4}NiO_2$, ~ 32 K for $Li_{2/3}NiO_2$, and ~ 10.5 K for $Li_{3/5}NiO_2$. As T decreases from T_N, f_{IC} ($\equiv \omega_{IC}/2\pi$) increases with decreasing slope (df_{IC}/dT) and finally reaches around 22 MHz for $LiNiO_2$ (~ 33 MHz for $Li_{3/4}NiO_2$, ~ 30 MHz for $Li_{2/3}NiO_2$, and ~ 14 MHz for $Li_{3/5}NiO_2$) at the lowest T measured, as expected for the order parameter of the IC-AF (IC-SDW) state. Considering the "1/3 tail" component due to the powder average, the normalized A_{IC} suggests that almost the whole sample is in the IC-AF state below ~ 10 K for $LiNiO_2$ (~ 30 K for $Li_{3/4}NiO_2$, ~ 25 K for $Li_{2/3}NiO_2$, and ~ 5 K for $Li_{3/5}NiO_2$).

Although $T_m=10$ K was determined by χ measurements with $H=10$ Oe [11 K with $H=100$ Oe, see Fig. 6(d)], the present μ^+SR data yield that $T_N^{mid}=16$ K with static order appearing below 12 K for the almost stoichiometric $LiNiO_2$.

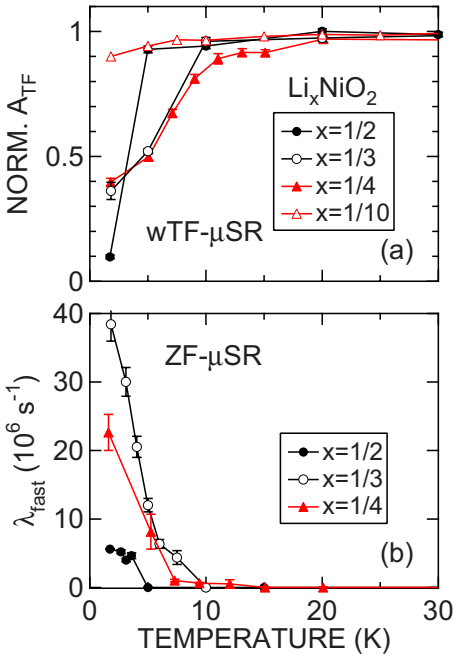

FIG. 7. (Color online) Temperature dependences of (a) normalized wTF asymmetry ($N_{A_{TF}}$) and (b) relaxation rate (λ_{fast}) for Li_xNiO_2 with $0.1 \leq x \leq 1/2$. The data were obtained by fitting the wTF spectrum using an exponential damped cosine oscillation $A_{TF}\exp(-\lambda_{TF}t)\cos(\omega_{TF}t+\phi)$ and the ZF spectrum using only the second and third terms of Eq. (1). The composition (Li/Ni ratio) determined by an ICP analysis for the samples with $x=1/2$, 1/3, 1/4, and 1/10 is 0.50, 0.37, 0.24, and 0.06, respectively.

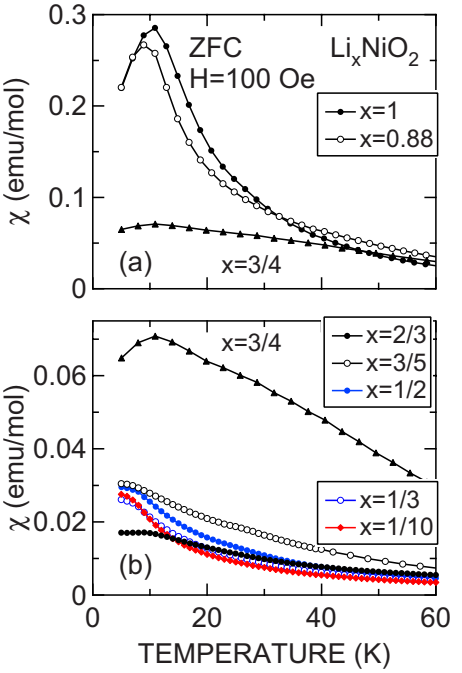

FIG. 8. (Color online) Temperature dependence of χ for Li_xNiO_2 with $0.1 \leq x \leq 1$ measured in ZFC mode with $H=100$ Oe.

Due to the wide distribution of the internal field observed, which results in a large λ_{IC} even at 1.6 K, it would be very difficult to detect static order by other techniques. In the previous μ^+SR experiment on $LiNiO_2$, the early time domain and the low T regime were not explored in enough detail to detect the ordering below 10 K.[5]

B. Li_xNiO_2 with $x \leq 3/5$

The ZF spectra for $Li_{1/2}NiO_2$, $Li_{1/3}NiO_2$, and $Li_{1/4}NiO_2$ exhibit a simple relaxation due to fluctuating moments, but the relaxation rate of $Li_{1/2}NiO_2$ is smaller than those of $Li_{1/3}NiO_2$ and $Li_{1/4}NiO_2$ [see Fig. 7(b)], suggesting a possible Li^+ ordering and/or charge ordering similar to the case of $Na_{0.5}CoO_2$.[34–36] The ZF spectrum for $Li_{0.1}NiO_2$ is almost time independent, which is consistent with the fact that, as x decreases from 1, the magnetic Ni^{3+} ions are converted to nonmagnetic Ni^{4+} ions ($t_{2g}^6, S=0$) (Ref. 37) to finally reach $Li_0Ni^{4+}O_2$. As seen in Fig. 7(a), the wTF measurements suggest a bulk magnetic transition with $T_N^{mid}=4$ K for $x=1/2$, 6 K for $x=1/3$, and 6.5 K for $x=1/4$. This indicates that these three samples exhibit a transition from the high-T paramagnetic phase to the low-T static disordered phase, i.e., a spin-glass-like phase at T_f, as in the case for the related compounds with the CoO_2 plane.[38]

C. Comparison with χ

For the Li_xNiO_2 samples with $x<1$, all the $\chi_{ZFC}(T)$ curves exhibit a clear cusp around 10 K ($=T_m$) regardless of the value of x, different from T_N^{mid} determined by wTF-μ^+SR (see Fig. 8). This means that T_m is induced by a minor component (below a few percent) in the sample, probably due to a very small amount of Ni ions at the $3b$ site. We wish therefore to emphasize that, since the cusp does not reflect the bulk magnetism, it is very hard or, in some case, may even be misleading to investigate the magnetic nature of Li_xNiO_2 only by χ measurements. In other words, μ^+SR is the most suitable technique for such purpose.

Figure 9 shows the T dependence of χ^{-1} for Li_xNiO_2 measured in field-cooling (FC) mode with $H=10$ kOe in order to study its macroscopic magnetic nature as a function of x. Roughly speaking, the $\chi^{-1}(T)$ curve for the samples with $x>0.5$ exhibits a linear T dependence above 100 K, while that for the $x \leq 1/2$ samples shows a nonlinear, i.e., a convex-type T dependence. A Curie-Weiss fit in the T range between 200 and 350 K yields a positive Θ for all x range down to 1/10, although μ_{eff} decreases monotonically with decreasing x as expected [see Figs. 9(b) and 9(c)]. Interestingly, as x decreases from 1, Θ increases from ~40 to ~55 K at around $x=0.8$ and then Θ decreases down to ~15 K at $x=0.5$. Below $x=0.5$, Θ seems to increase again with decreasing x, although it is difficult to estimate it precisely from the convex-shaped $\chi^{-1}(T)$ curve. In other words, the $\Theta(x)$ curve exhibits a broad maximum at $x=0.8$, around which μ^+SR detects a clear oscillation at low T. Actually, there is a good correlation between Θ and T_N (T_f) determined by μ^+SR, as seen in Fig. 9(b). This means that the static magnetic order is induced mainly by a FM interaction, although the spontaneous magnetization has not been observed at low T for all the samples.

IV. DISCUSSION

Since the Li-deficient samples are unstable in air and it is hard to prepare a proper amount for ND measurements

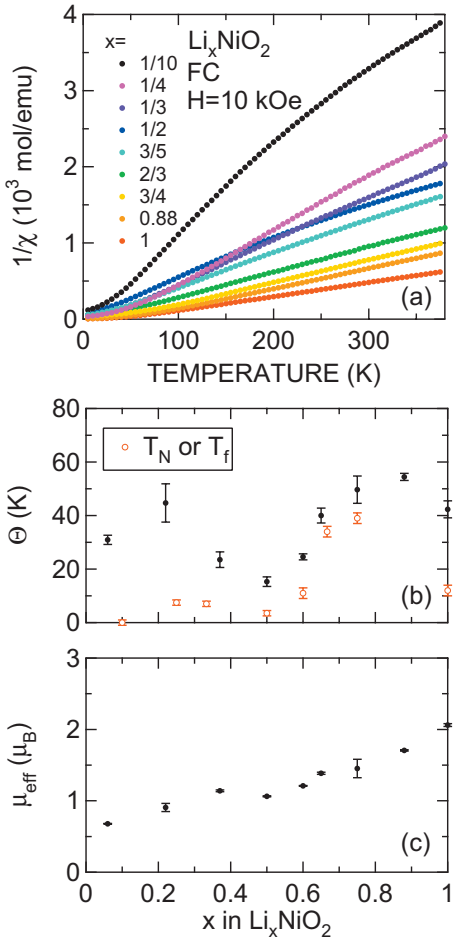

FIG. 9. (Color) (a) Temperature dependence of χ^{-1} for Li_xNiO_2 with $0.1 \leq x \leq 1$ measured in FC mode with $H=10$ kOe, the relationship between (b) Weiss temperature (Θ) and x and (c) the effective magnetic moment (μ_{eff}) and x. Θ and μ_{eff} were obtained by fitting the $\chi^{-1}(T)$ curve in the T range between 200 and 350 K using a Curie-Weiss formula $\chi=\chi_0+C/(T-\Theta)$. Here, χ_0 is a T-independent χ in order to fit the convex-shape $\chi^{-1}(T)$ curve. In (b), T_N and T_f determined by the wTF-μ^+SR measurements are also plotted for comparison.

(10 cm^3), information on their magnetic structure is currently unavailable. Here, we discuss their magnetic structure in relation to the present μ^+SR and χ results using two possible structures, namely, A-type AF order with an IC modulation in the NiO_2 plane or, alternatively, IC-SDW order in the NiO_2 plane.

According to the above χ measurements, the predominant interaction between the Ni moments is most likely FM. This would directly lead to FM order of the Ni moments in the NiO_2 plane. The absence of bulk ferromagnetism suggests that the FM-ordered plane is coupled antiferromagnetically, i.e., A-type AF order as for $NaNiO_2$. Past magnetizations and ND measurements on $NaNiO_2$ have shown that the intraplane FM coupling constant (J_{FM}) is 29 K and the interplane AF coupling constant (J_{AF}) is −1.9 K,[12,14,39] but with $\Theta=35$ K and $T_N=20$ K. Since this Θ is comparable to those for Li_xNiO_2 with $x \geq 3/5$ [see Fig. 9(b)], it is reasonable to assume the similar values of J_{FM} and J_{AF} for Li_xNiO_2, resulting in A-type AF order at low T. This is also consistent with the fact that both the $T_N(x)$ and $\Theta(x)$ curves show their maximum at around $x=0.8$.

In order to explain the IC nature detected by μ^+SR, we need to introduce an IC modulation of the ordered moments in the plane because such modulation is very unlikely to appear along the c_{H} axis. Here, we should note that the direction of the ordered moment ($\mu_{\text{ord}}=0.97\ \mu_B$) for $NaNiO_2$ is canted by ~10° from the c_{H} direction.[13] The in-plane component (0.18 μ_B) also aligns ferromagnetically along the a_{H} axis in the plane, but antiferromagnetically between the neighboring planes.[13] Assuming that μ_{ord} is also canted for $LiNiO_2$, FM order of the in-plane component would be strongly perturbed by the Ni ions in the Li layer because such Ni ions induce an additional interplane interaction through the Ni_{3a}-Ni^{2+}_{3b}-Ni_{3a} coupling in $[Li^+_{1-z}Ni^{2+}_z]_{3b}[Ni^{3+}_{1-z}Ni^{2+}_z]_{3a}[O_2]_{6c}$. As a result, although the Ni moments mainly align along the c_{H} axis, the in-plane component would form a spin-flow pattern, which was predicted for the vortex-lattice state on the 2DTL,[40] around the Ni_{3a} ions located just below or above the Ni^{2+}_{3b} ions in the Li layer. Furthermore, since the Ni^{2+}_{3b} ions distribute randomly in the Li layer so as to minimize electrostatic repulsion, the obtained spin-flow pattern would be expected to be incommensurate to the 2DTL.

For $NaNiO_2$, although $\mu_{\text{eff}}=1.85\ \mu_B$,[41] μ^+SR measurements showed that $f_{\text{AF}}(0\ \text{K}) \sim 64$ MHz.[15] This value is two or three times higher than those for Li_xNiO_2, while μ_{eff} is comparable to that for $LiNiO_2$ (~2.0 μ_B). This means that either μ_{ord} for $LiNiO_2$ is smaller than that for $NaNiO_2$ (0.97 μ_B) or that the angle between μ_{ord} and c_{H} plane for $LiNiO_2$ is smaller than that for $NaNiO_2$ (~100°). Since the distance between the two adjacent NiO_2 planes is 0.473 nm for $LiNiO_2$ (Ref. 6) and 0.52 nm for $NaNiO_2$,[14] the canting angle of μ_{ord} for $LiNiO_2$ is naturally expected to be larger than that for $NaNiO_2$, resulting in a larger in-plane component of μ_{ord}. Therefore, IC order of the in-plane component would decrease the internal magnetic field, as observed by the present μ^+SR data.

If the intraplane coupling is AF, theoretical studies based on the Hubbard model have predicted the appearance of IC-SDW order on the 2DTL (Refs. 42 and 43) as a function of U/t and the spin concentration (n), where U is the on-site repulsion and t is the electron transfer. When $n=1/2$, as U/t increases from 0, a paramagnetic phase changes to an IC-SDW phase at $U/t=3.97$ and then to a classical 120° AF phase at $U/t=5.27$. We could then deduce that $3.97 \leq U/t \leq 5.27$ for $LiNiO_2$, although the local-orbital ordering hinders the formation of long-range order detectable by ND and/or NMR measurements.[6] The decrease in n from 1/2 is thought to suppress geometrical frustration, resulting in further stabilization of the IC-SDW phase for Li_xNiO_2 with $x=3/4$. The decrease in T_N and f_{IC} (and increase in λ_{IC}) with further lowering x could be explained by the decrease in the spin concentration, i.e., the number density of the nearest neighboring Ni moments. This could be, therefore, a reasonable explanation for the change in magnetic nature of Li_xNiO_2 with decreasing x from 1 to 3/5, although a theoretical treatment to describe the magnetic phases formed on the 2DTL as a function of n and U/t is not currently available.

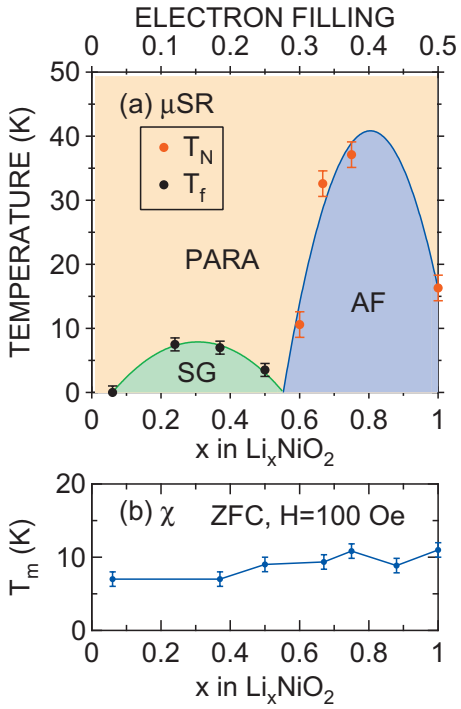

FIG. 10. (Color) (a) Schematic phase diagram of Li_xNiO_2 determined by μ^+SR and the x dependences of (b) T_m, which corresponds to the cusp T in the $\chi(T)$ curve measured in ZFC mode with $H=100$ Oe. Here, T_N and T_f are the T at which $N_{A_{TF}}(T)=0.5$. In (a), AF stands for an incommensurate antiferromagnetic ordered phase and SG a spin-glass-like phase. The phase boundary between AF and SG phases is still ambiguous at present.

Considering the overall results, including past work, we conclude that A-type AF order with an in-plane IC modulation is a reasonable description of the ground state for $LiNiO_2$. The Ni ions in the Li layer, however, naturally hinder the formation of long-range order, which would be detectable by ND and/or NMR whether the additional interplane interaction is FM or AF.[15] On the other hand, since muons mainly sense the local magnetic field generated by the nearest neighboring moments, μ^+SR has provided information on static but short-range magnetic order for Li_xNiO_2 with $3/5 \leq x \leq 1$. This conclusion is, therefore, consistent with the ground state for $LiNiO_2$ proposed by NMR, i.e., a spin-liquid state with short-range FM correlations.[4]

Finally, we present a schematic magnetic phase diagram for Li_xNiO_2 based on the present μ^+SR results (see Fig. 10). A dome-shaped AF phase region exists in the x range between ~ 0.55 and 1, whereas the SG-like phase appears below $x \sim 0.55$, and the paramagnetic phase is stable below $x=0.1$, down to the lowest T measured. The dome-shaped boundary of the AF phase indicates the competition between the spin concentration and the FM interaction on the 2DTL of the NiO_2 plane.

V. SUMMARY

Thanks to the unique power of μ^+SR, we have found the formation of static magnetic order, i.e., A-type AF order with an in-plane IC modulation, for Li_xNiO_2 with $x=3/4$ and 2/3 below around 35 K, while the $\chi(T)$ curve exhibits no anomalies in the same T range. The careful analysis of the ZF spectrum for $LiNiO_2$ and $Li_{3/5}NiO_2$ reveals that their ground states are also most likely an A-type AF ordered phase, but short ranged. On the other hand, Li_xNiO_2 with $x \leq 1/2$ is found to enter into a spin-glass-like phase at low T, but $Li_{0.1}NiO_2$ is paramagnetic down to the lowest T measured. These results are explained by competition between the concentration of FM coupled spins and J_{FM} on the NiO_2 triangular lattice.

Our systematic μ^+SR study on Li-battery materials has clarified their interesting microscopic magnetic and structural natures,[30,44,45] which are very sensitive to the Li content. This is because such materials include a rigid lattice as a skeleton, which provides open paths for mobile Li^+ ions. Since the skeleton is usually formed by a two-dimensional triangular lattice, Kagome-lattice, or spinel (pyrochlore) lattice of transition metals, the combination of electrochemical Li-deintercalation techniques with μ^+SR is a powerful method to detect the change in magnetic nature of these frustrated systems as a function of the spin concentration, as illustrated by the present results in Fig. 10.

ACKNOWLEDGMENTS

This work was performed at the Swiss Muon Source, Paul Scherrer Institut, Villigen, Switzerland. We thank the staff of PSI for help with the μ^+SR experiments. We also appreciate J. H. Brewer of the University of British Columbia and E. J. Ansaldo of TRIUMF for discussion, S. Kohno of OCU for sample preparation, and Y. Kondo of TCRDL for compositional analyses. K.M., Y.I., and J.S. are partially supported by the KEK-MSL Inter-University Program for Overseas Muon Facilities. This work is supported by Grant-in-Aid for Scientific Research (B) (Grant No. 19340107) MEXT, Japan.

*e0589@mosk.tytlabs.co.jp

[1] T. A. Hewston and B. L. Chamberland, J. Phys. Chem. Solids **48**, 97 (1987).

[2] J. Molenda, P. Wilk, and J. Marzec, Solid State Ionics **119**, 19 (1999).

[3] K. Hirakawa, H. Kadowaki, and K. Ubukoshi, J. Phys. Soc. Jpn. **54**, 3526 (1985).

[4] Y. Kitaoka, T. Kobayashi, A. Koda, H. Wakabayashi, Y. Niino, H. Yamakage, S. Taguchi, K. Amaya, K. Yamaura, M. Takano, A. Hirano, and R. Kanno, J. Phys. Soc. Jpn. **67**, 3703 (1998).

[5] T. Chatterji, W. Henggeler, and C. Delmas, J. Phys.: Condens. Matter **17**, 1341 (2005).

[6] J.-H. Chung, Th. Proffen, S. Shamoto, A. M. Ghorayeb, L. Croguennec, W. Tian, B. C. Sales, R. Jin, D. Mandrus, and T.

Egami, Phys. Rev. B **71**, 064410 (2005).
[7] J. N. Reimers, J. R. Dahn, J. E. Greedan, C. V. Stager, G. Liu, I. Davidson, and U. Von Sacken, J. Solid State Chem. **102**, 542 (1993).
[8] A. Rougier, C. Delmas, and G. Chouteau, J. Phys. Chem. Solids **57**, 1101 (1996).
[9] J. B. Goodenough, D. G. Wickham, and W. J. Croft, Phys. Chem. Solids **5**, 107 (1958).
[10] M. Takano, R. Kanno, and T. Takeda, Mater. Sci. Eng., B **63**, 6 (1999).
[11] Y. Takahashi, J. Akimoto, Y. Gotoh, K. Kawaguchi, and S. Mizuta, J. Solid State Chem. **160**, 178 (2001).
[12] A. J. W. Reitsma, L. F. Feiner, and A. M. Olés, New J. Phys. **7**, 121 (2005).
[13] C. Darie, P. Bordet, S. de Brion, M. Holzapfel, O. Isnard, A. Lecchi, J. E. Lorenzo, and E. Suard, Eur. Phys. J. B **43**, 159 (2005).
[14] M. J. Lewis, B. D. Gaulin, L. Filion, C. Kallin, A. J. Berlinsky, H. A. Dabkowska, Y. Qiu, and J. R. D. Copley, Phys. Rev. B **72**, 014408 (2005).
[15] P. J. Baker, T. Lancaster, S. J. Blundell, M. L. Brooks, W. Hayes, D. Prabhakaran, and F. L. Pratt, Phys. Rev. B **72**, 104414 (2005).
[16] H. Kikuchi, H. Nagasawa, M. Mekata, Y. Fudamoto, K. M. Kojima, G. M. Luke, Y. J. Uemura, H. Mamiya, and T. Naka, Hyperfine Interact. **120-121**, 623 (1999).
[17] E. Wawrzyńska, R. Coldea, E. M. Wheeler, I. I. Mazin, M. D. Johannes, T. Sörgel, M. Jansen, R. M. Ibberson, and P. G. Radaelli, Phys. Rev. Lett. **99**, 157204 (2007).
[18] T. Lancaster, S. J. Blundell, P. J. Baker, M. L. Brooks, W. Hayes, F. L. Pratt, R. Coldea, T. Sörgel, and M. Jansen, Phys. Rev. Lett. **100**, 017206 (2008).
[19] H. Yoshida, Y. Muraoka, T. Sörgel, M. Jansen, and Z. Hiroi, Phys. Rev. B **73**, 020408(R) (2006).
[20] J. Sugiyama, Y. Ikedo, K. Mukai, J. H. Brewer, E. J. Ansaldo, G. D. Morris, K. H. Chow, H. Yoshida, and Z. Hiroi, Phys. Rev. B **73**, 224437 (2006).
[21] A. M. Oles, L. F. Feiner, and J. Zaanen, Phys. Rev. B **61**, 6257 (2000).
[22] F. Reynaud, D. Mertz, F. Celestini, J.-M. Debierre, A. M. Ghorayeb, P. Simon, A. Stepanov, J. Voiron, and C. Delmas, Phys. Rev. Lett. **86**, 3638 (2001).
[23] M. V. Mostovoy and D. I. Khomskii, Phys. Rev. Lett. **89**, 227203 (2002).
[24] F. Vernay, K. Penc, P. Fazekas, and F. Mila, Phys. Rev. B **70**, 014428 (2004).
[25] L. Petit, G. M. Stocks, T. Egami, Z. Szotek, and W. M. Temmerman, Phys. Rev. Lett. **97**, 146405 (2006).
[26] T. Ohzuku, A. Ueda, and M. Nagayama, J. Electrochem. Soc. **140**, 1862 (1993).
[27] W. Li, J. N. Reimers, and J. R. Dahn, Solid State Ionics **67**, 123 (1993).
[28] C. Chazel, M. Ménétrier, L. Croguennec, and C. Delmas, Inorg. Chem. **45**, 1184 (2006).
[29] E. Chappel, M. D. Néñez-Regueiro, G. Chouteau, A. Sulpice, and C. Delmas, Solid State Commun. **119**, 83 (2001).
[30] K. Mukai, Y. Ikedo, H. Nozaki, J. Sugiyama, K. Nishiyama, D. Andreica, A. Amato, P. L. Russo, E. J. Ansaldo, J. H. Brewer, K. H. Chow, K. Ariyoshi, and T. Ohzuku, Phys. Rev. Lett. **99**, 087601 (2007).
[31] G. M. Kalvius, D. R. Noakes, and O. Hartmann, in *Handbook on the Physics and Chemistry of Rare Earths*, edited by K. A. Gschneidner, Jr., L. Eyring, and G. H. Lander (Elsevier, Amsterdam, 2001), Vol. 32, Chap. 206, and references cited therein.
[32] P. C. M. Gubbens, D. Visser, P. Dalmas de Réotier, A. Yaouanc, A. Amato, S. P. Cottrell, and P. J. C. King, Physica B (Amsterdam) **374-375**, 160 (2006).
[33] G. Grüner, *Density Waves in Solids* (Addison-Wesley, Reading, 1994), Chap. 4.
[34] M. L. Foo, Y. Wang, S. Watauchi, H. W. Zandbergen, T. He, R. J. Cava, and N. P. Ong, Phys. Rev. Lett. **92**, 247001 (2004).
[35] H. W. Zandbergen, M. L. Foo, Q. Xu, V. Kumar, and R. J. Cava, Phys. Rev. B **70**, 024101 (2004).
[36] Q. Huang, M. L. Foo, J. W. Lynn, H. W. Zandbergen, G. Lawes, Y. Wang, B. H. Toby, A. P. Ramirez, N. P. Ong, and R. J. Cava, J. Phys.: Condens. Matter **16**, 5803 (2004).
[37] H. Ikeno, I. Tanaka, Y. Koyama, T. Mizoguchi, and K. Ogasawara, Phys. Rev. B **72**, 075123 (2005).
[38] J. Sugiyama, J. H. Brewer, E. J. Ansaldo, H. Itahara, T. Tani, M. Mikami, Y. Mori, T. Sasaki, S. Hébert, and A. Maignan, Phys. Rev. Lett. **92**, 017602 (2004).
[39] E. Chappel, M. D. Néñez-Regueiro, G. Chouteau, O. Isnard, and C. Darie, Eur. Phys. J. B **17**, 615 (2000).
[40] M. Fujita, T. Nakanishi, and K. Machida, Phys. Rev. B **45**, 2190 (1992).
[41] E. Chappel, M. D. Néñez-Regueiro, F. Dupont, G. Chouteau, C. Darie, and A. Sulpice, Eur. Phys. J. B **17**, 609 (2000).
[42] H. R. Krishnamurthy, C. Jayaprakash, S. Sarker, and W. Wenzel, Phys. Rev. Lett. **64**, 950 (1990).
[43] M. Fujita, M. Ichimura, and K. Nakao, J. Phys. Soc. Jpn. **60**, 2831 (1991).
[44] J. Sugiyama, H. Nozaki, J. H. Brewer, E. J. Ansaldo, G. D. Morris, and C. Delmas, Phys. Rev. B **72**, 144424 (2005).
[45] J. Sugiyama, K. Mukai, Y. Ikedo, P. L. Russo, T. Suzuki, I. Watanabe, J. H. Brewer, E. J. Ansaldo, K. H. Chow, K. Ariyoshi, and T. Ohzuku, Phys. Rev. B **75**, 174424 (2007).